AIP Advances

Numerical research on the cavitation effect induced by underwater multi-point explosion near free surface

Cite as: AIP Advances **13**, 015021 (2023); https://doi.org/10.1063/5.0136546
Submitted: 27 November 2022 • Accepted: 03 January 2023 • Published Online: 19 January 2023

Jun Yu (余俊), **Hai-tao Li** (李海涛), **Zhen-xin Sheng** (盛振新), **et al.**

Numerical research on the cavitation effect induced by underwater multi-point explosion near free surface

Cite as: AIP Advances 13, 015021 (2023); doi: 10.1063/5.0136546
Submitted: 27 November 2022 • Accepted: 3 January 2023 •
Published Online: 19 January 2023

Jun Yu (余俊),[1,2,a)] Hai-tao Li (李海涛),[1] Zhen-xin Sheng (盛振新),[1] Yi Hao (郝轶),[1] and Jian-hu Liu (刘建湖)[1,2]

AFFILIATIONS

[1] China Ship Scientific Research Center, Wuxi 214082, China
[2] Taihu Laboratory of Deep-sea Technological Science, Wuxi 214082, China

[a)] **Authors to whom correspondence should be addressed:** yujun@cssrc.com.cn and feiyue617@163.com

ABSTRACT

In this study, the cavitation effect induced by two charges in underwater explosions near free surfaces is numerical researched by two dimensional compressible multiphase fluids based on a four-equation system with a phase transition model. The occurrence of the generation, development, and collapse of cavitation in two-charge underwater explosions near free surfaces can be captured directly. The detailed density, pressure, and vapor volume fraction contours during the interaction process are obtained and can better reveal the characteristic underlying the cavitation, free surface, and explosion bubbles. Numerical results reveal that the cavitation domain has expanded to an area much deeper than the explosion bubble location in two-charge underwater explosions, which should be paid enough attention due to its influence on the input load of underwater structures. The detailed density and pressure contours during the interaction process can also be captured and can better reveal the mechanism underlying the explosion bubble, cavitation, and surface wave dynamics. The present results can expand the currently limited database of multiphase fluid in underwater explosions and also provide new insights into the strong nonlinear interaction between underwater explosion and cavitation, which provides a deep understanding of multi-point explosions.

I. INTRODUCTION

Underwater explosions (UNDEXs) have been applied to many fields, such as seafloor mining, underwater obstacle suppression, and military applications. The effects of underwater explosions on the nearby structures initially are a high-pressure shock wave and cavitation collapse. In the study of the underwater explosion phenomenon, water is supposed to be compressible and unable to sustain shear stress. Underwater explosions can be divided into three important stages: charge detonation, shock wave propagation, and bubble pulsation.[1–4] Just after the detonation of the charge, the shock wave and explosion bubble will appear in water. The propagation speed of the shock wave in water is very fast, but its intensity attenuates slowly. The explosive products will form gas bubbles with high pressure and high density. Due to the transient impact effect of the shock wave and explosion bubble in the process of underwater explosions, there is a strong demand for research on the characteristics of underwater explosions in the field of shock damage and protection design, which has attracted the attention of many scholars.

In order to enhance the destructive power and investigate the dynamics characteristics of underwater explosions, a lot of research on multi-point array explosions has been carried out. The explosion of two charges at the bottom of a shallow layer of water is simulated, and the effect on the shock wave propagation and interaction between charges and the bottom is researched.[5] It is found that the maximum value of the shock wave pressure and its impulse decreased. Two gaseous bubbles merging into a single coalesced bubble are investigated by a boundary integral method in underwater explosions.[6] When the critical thickness defined as the coalescence criterion based on experimental results was satisfied, the bubbles would merge into one. The interaction of multiple bubbles has a significant influence on the motion of the free surface

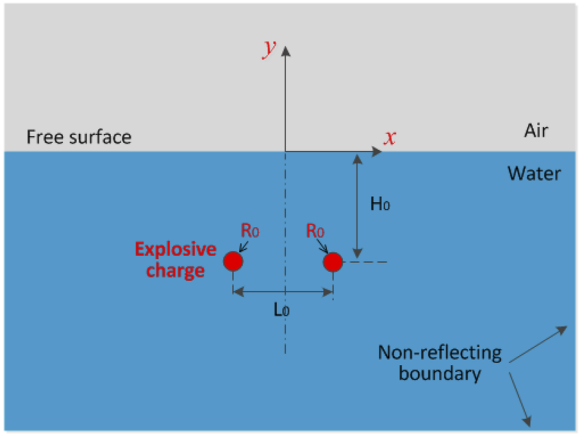

FIG. 1. Schematic diagram of two charges placed horizontally in underwater explosions near free surfaces.

and induced the formation of coalesced bubbles.[7] The underwater explosion parameters of multi-point array explosions are measured through an underwater explosion test, and the multi-shock wave collision of array explosion can be approximated to a linear superposition in some cases. In addition, the interaction of the delayed shock wave can be considered as due to the increase in the shock wave baseline.[8] Near-field pressure evolution of shock waves and high-pressure zones between two detonation tubes is numerically studied, and the formation, intersection, and interaction of shock waves are revealed.[9] The strong nonlinear interaction of two underwater explosion bubbles with a free surface are numerically researched by an axisymmetric fully compressible three-phase homogeneous model, and the detailed pressure and velocity contours during the interaction process can be obtained and revealed to understand the mechanism underlying the bubbles and free surface dynamics.[10]

These research studies mainly focus on the shock wave and explosion bubble effect under multi-point charges, but there are few studies on the cavitation effect. The strong nonlinear interactions among the water, explosion bubble, cavitation, and air have an important influence on the shock wave propagation and bubble pulsation. The cavitation domain induced by underwater explosions near free surfaces occupies a large area in water and must be properly dealt with. A very low pressure in the cavitation zone is required to be simulated by coupling to a cavitation model. Some one-fluid models that have been developed to simulate the cavitation are the cut-off mode[11] and the Schmidt model.[12] The isentropic one-fluid model was proposed to treat the fluid as a mixture comprising isentropic vapor and liquid phases.[13] The modified Schmidt model was created to improve the application of the Schmidt model to unsteady transient cavitation flow.[14] Another new isentropic cavitation model was proposed to research underwater explosion cavitation based on a reduced five-equation system.[15] The biggest disadvantage of one-fluid models is that they have lost the ability to capture the vapor–liquid two-phase transition in the generation of cavitation. In order to overcome this drawback, two-fluid models have been established in the past decade. Pelanti and Shyue[16,17] developed a new multiphase model on the basis of the six-equation system, which could efficiently deal with interfaces, cavitation, and evaporation waves. A phase transition model based on a four-equation system was used to deal with the thermodynamic equilibrium between a liquid phase and its corresponding vapor phase.[18,19] The four-equation model with phase transition has been used to investigate the cavitation evolvement in underwater explosion, and the physical characteristics of the flow field in the cavitation domain can be captured.[20–23] Another phase transition model base on the five-equation system using temperature and chemical relaxation with the monotonic mixture speed of sound was built by Zhang.[24]

To our best knowledge, further research on the strong nonlinear interactions between two charges and cavitation is necessary and compressible multiphase fluids with the two-fluid phase transition model has not been reported yet. In this study, the four-equation system with a phase transition model[19,21] is employed to investigate the cavitation effect induced by two-charge explosions near free surfaces. The strong nonlinear interaction among the multiphase fluids including explosion bubbles, cavitation, water, and air can be revealed. The remainder of this paper is organized as follows: numerical methods with governing equations, numerical results for the cavitation effect in two-charge underwater explosions near free surfaces, and a conclusion with scope of future research.

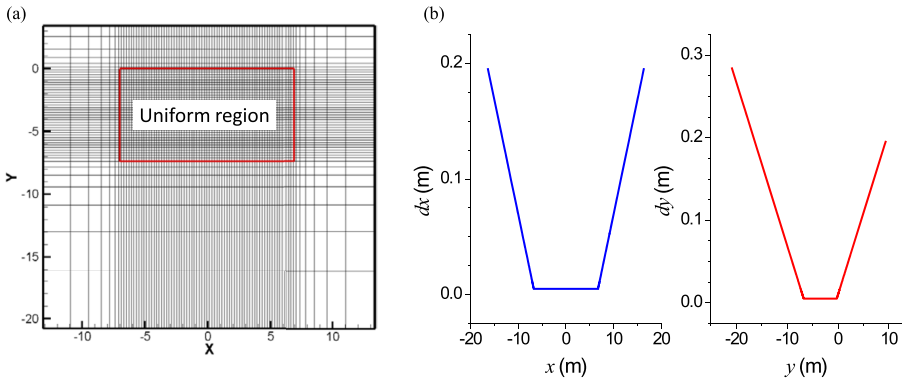

FIG. 2. Mesh strategy of the fluid domain; every one in 20 of the lines is plotted in the left figure (a) and grid length distribution of two normal directions is plotted in the right figure (b).

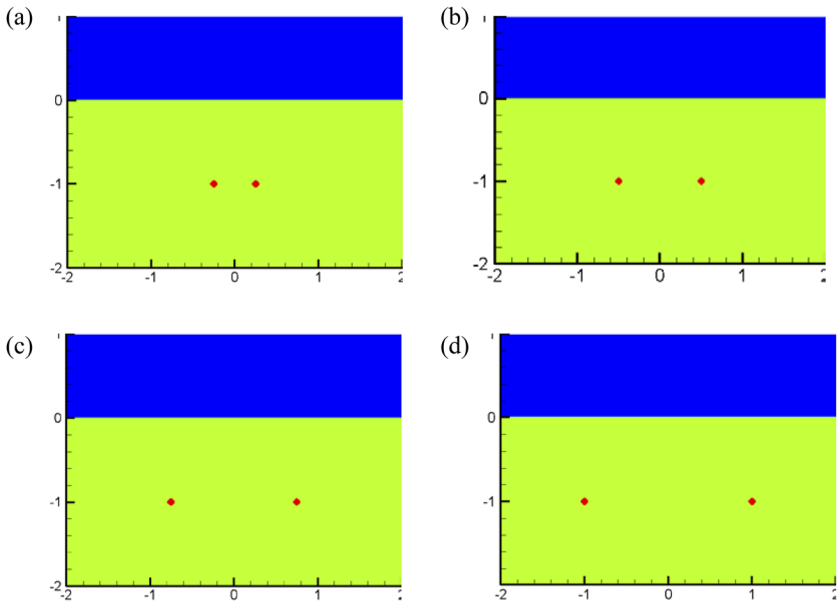

FIG. 3. Schematic of two-charge underwater explosions with R_0 = 0.04 m and H_0 = 1 m under different detonation distances: (a) L_0 = 0.5 m; (b) L_0 = 1.0 m; (c) L_0 = 1.5 m; (d) L_0 = 2.0 m.

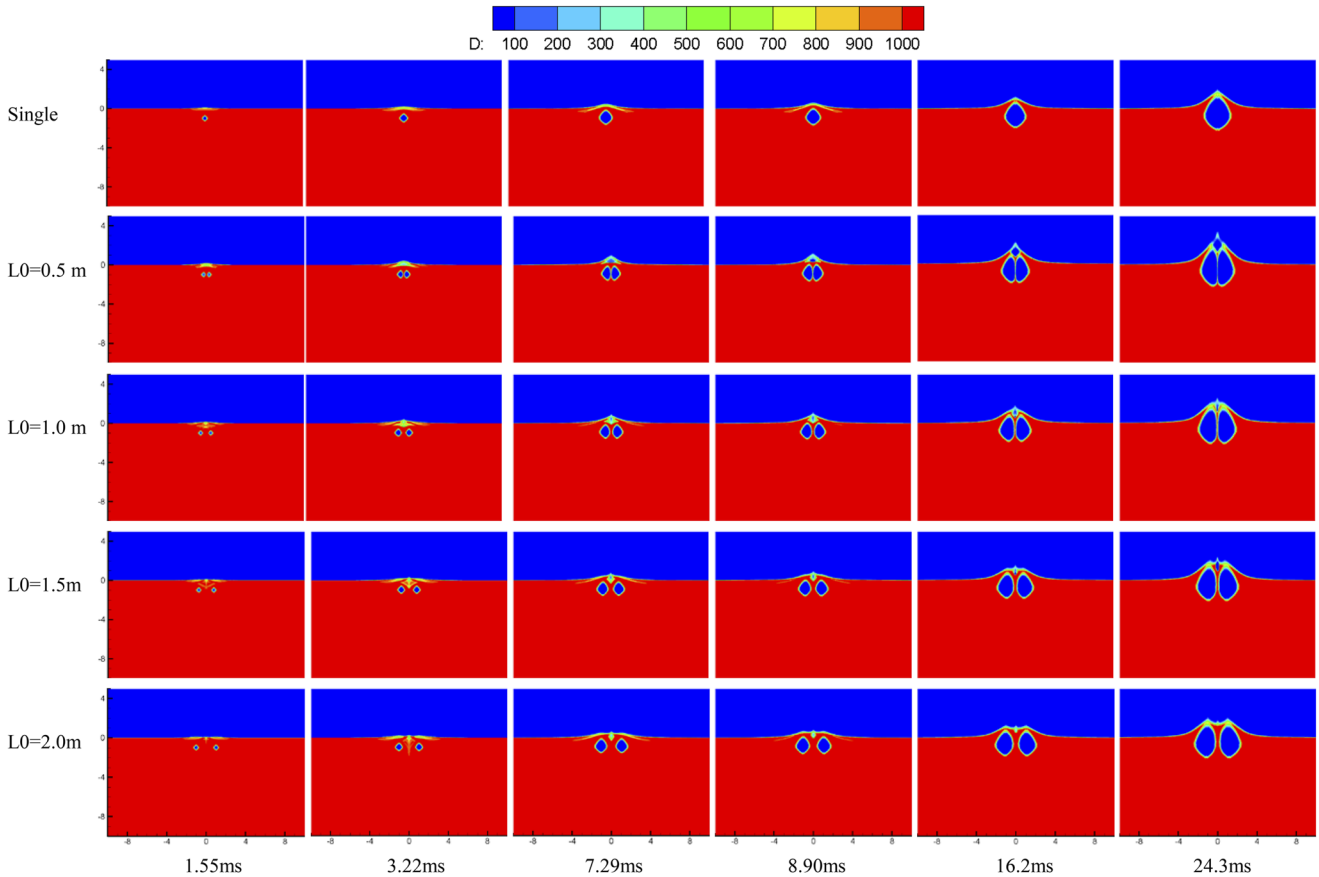

FIG. 4. Numerical results of the density contour plot at times of t = 1.55, 3.22, 7.29, 8.90, 16.2, and 24.3 ms (from left to right) with R_0 = 0.04 m and H_0 = 1 m under single charge and two charges with different detonation distances L_0 (from up to down).

II. PHYSICAL PROBLEM AND NUMERICAL METHOD

A. Physical problem

Underwater explosions induced by two charges near free surfaces are considered, as shown in Fig. 1. In this model, the two charges are of the same type and size, which are detonated instantly. R_0 is the initial radius of the charge, H_0 is the detonation depth, and L_0 is the distance between the two charges placed horizontally under the free surface. The computational domain consists of three main regions: explosion gas, water, and air. The nonreflection characteristic boundary conditions are applied to the other boundaries.

A two-dimensional model can simplify this physical problem and save the calculation time and resources, especially in large-scale applications. In the present study, the two-dimensional plane model is used to qualitatively study the two charges placed horizontally with different charge radii R_0 and detonation depths H_0 in Secs. III A and III B, and then the two-dimensional axisymmetric model is adopted to quantitatively investigate the two charges placed vertically in Sec. III C.

B. Numerical method

The mechanical essence of the above-mentioned physical problems is the motion process of explosion bubbles, water, air, and other fluids in underwater explosions. Therefore, the compressible multiphase flow model can be adopted for this research. The four-equation model for compressible multiphase flows reads[19]

$$\frac{\partial Q}{\partial t} + \frac{\partial F}{\partial x} + \frac{\partial G}{\partial y} = 0, \tag{1}$$

where $Q = [\rho, \rho u, \rho v, \rho E, \rho Y_k]^T$, $F = [\rho u, \rho u^2 + p, \rho uv, (\rho E + \rho)u, \rho Y_k u]^T$, $G = [\rho v, \rho uv, \rho v^2 + p, (\rho E + p)v, \rho Y_k v]^T$, ρ is the fluid density, u and v are velocity components of the x and y axis, respectively, p is the pressure, E is the total energy per unit mass, and Y_k is the mass fraction for the k-th species in the entire mixture fluid. The parameter k can be specified as follows: $k = 1$ for the liquid water phase, $k = 2$ for the vapor water phase, and $k = 3, \ldots, N$ for other fluids without phase transition. Both viscosity and thermal effect in the fluid are

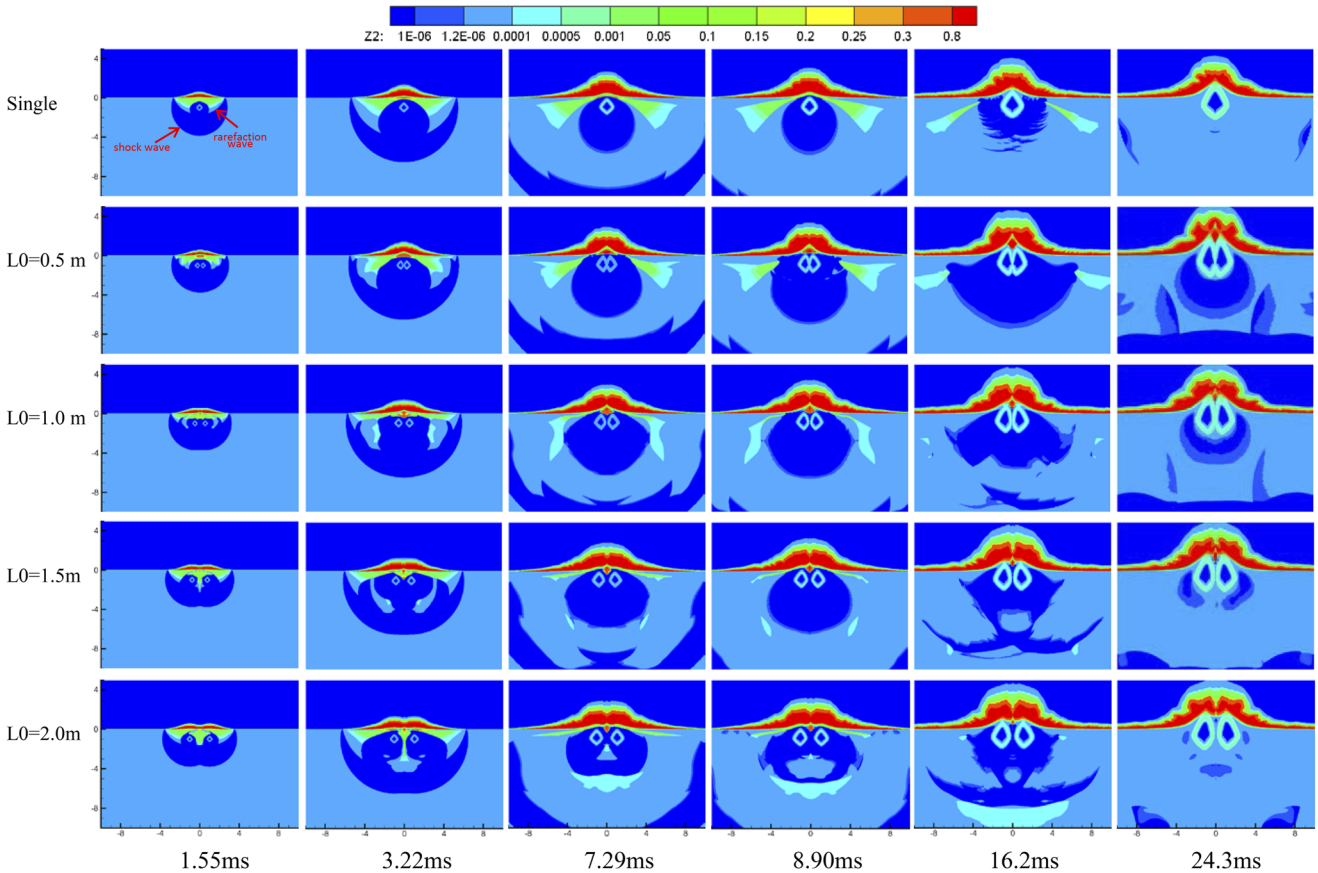

FIG. 5. Numerical results of the vapor volume fraction contour plot at times of t = 1.55, 3.22, 7.29, 8.90, 16.2, and 24.3 ms (from left to right) at R_0 = 0.04 m and H_0 = 1 m in the cases of single charge and two charges with different detonation distances L_0 (from up to down).

ignored here. The equation of state for each phase fluid is described by the Noble-Abel Stiffened-Gas (NASG) EOS.[25]

The four-equation system (1) does not take the mass transfer between the liquid water and its vapor phase into account. In other words, the liquid water and its vapor phase in the mixture solved by Eq. (1) are out of thermodynamic equilibrium. During the phase transition process, the mixture specific volume $v = 1/\rho$ and internal energy e do not vary under the assumption of constant pressure and constant velocity. The mass fractions for the liquid and its vapor phase remain constant, although the pressure and temperature vary and reach their equilibrium values (p^*, T^*), so that the phase transition model will change to compute the equilibrium state $(p^*, T^*, Y_{k=1,2})$ from the state (v, e, p, T, Y_k). Therefore, under the assumption of mechanical and thermal equilibrium, the mixture fluid satisfies[19,24]

$$\begin{cases} T = T_k, & p = p_k, \forall k, \\ v = \sum_{k=1}^{N} Y_k v_k, & e = \sum_{k=1}^{N} Y_k e_k. \end{cases} \tag{2}$$

This system contains four unknown variables with four equations, which can be solved by the Newton iterative method.

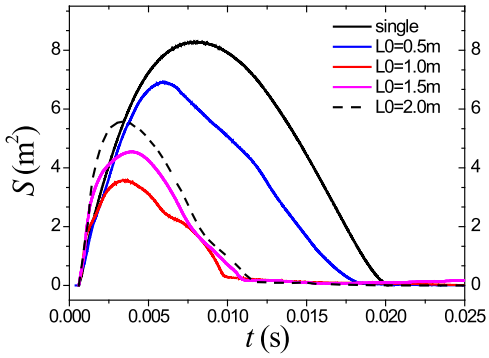

FIG. 7. Time-history curve of cavitation domain volume evolvement at $R_0 = 0.04$ m and $H_0 = 1$ m in the cases of single charge and two charges with different detonation distances L_0.

Therefore, to ensure that the final equilibrium state is (p^*, T^*), the phase transition model is saturated at each step. The numerical method of the multiphase compressible fluid model in this study has been previously validated by various cases involving phase transition in underwater explosion applications.[21–24]

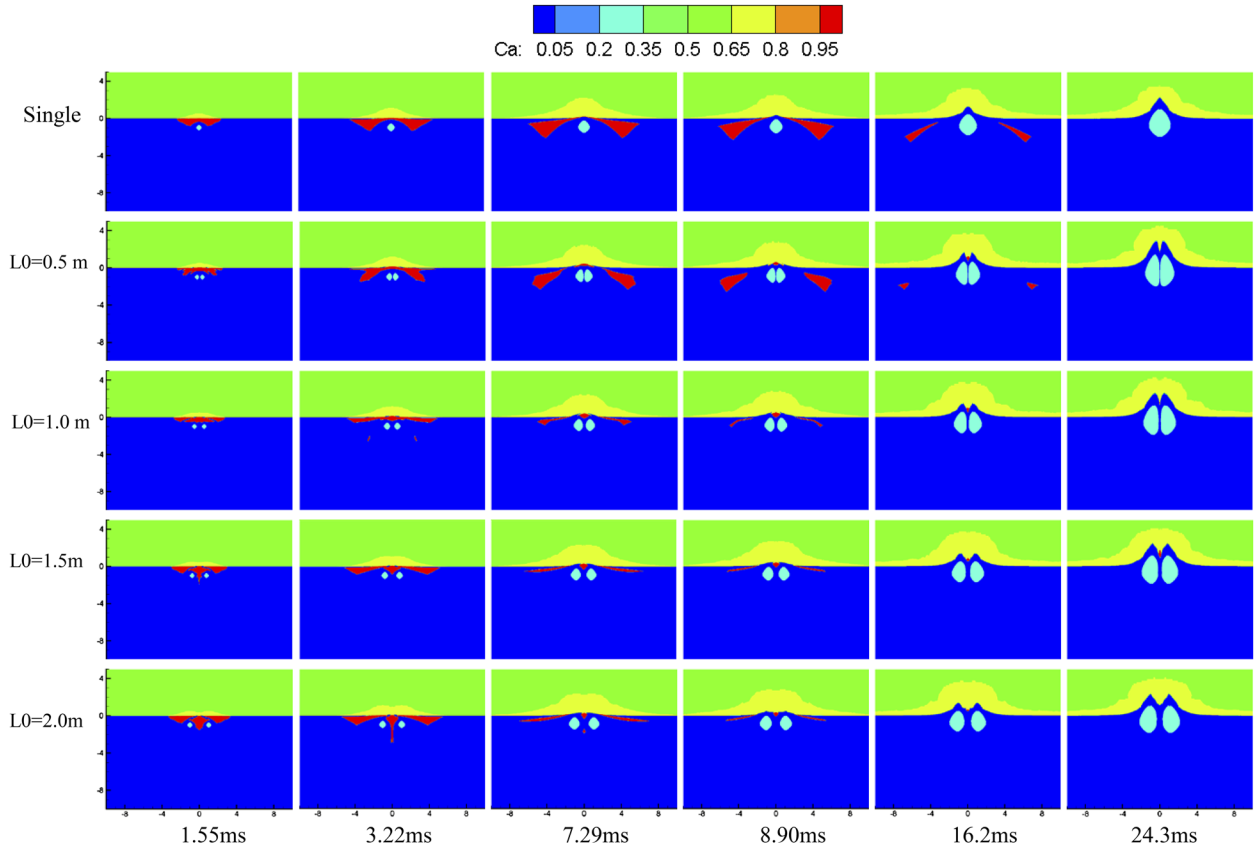

FIG. 6. Numerical results of the cavitation domain fraction contour plot at times of $t = 1.55$, 3.22, 7.29, 8.90, 16.2, and 24.3 ms (from left to right) at $R_0 = 0.04$ m and $H_0 = 1$ m in the cases of single charge and two charges with different detonation distances L_0 (from up to down). The red zones represent the cavitation area, and the green, blue, and light blue color zones are air, water, and the explosion bubble, respectively.

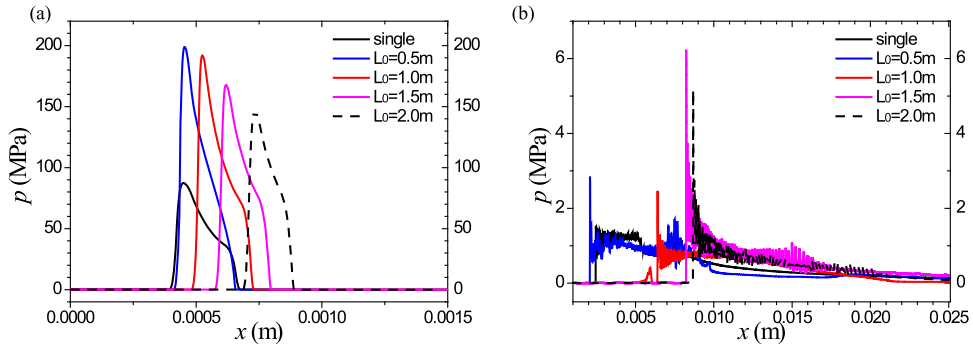

FIG. 8. Pressure time-history curves for the location of (0, −0.2) m at R_0 = 0.04 m and H_0 = 1 m in the cases of single charge and two charges with different detonation distances L_0. (a) The pressure at the shock wave stage. (b) The pressure at the cavitation pressure curve.

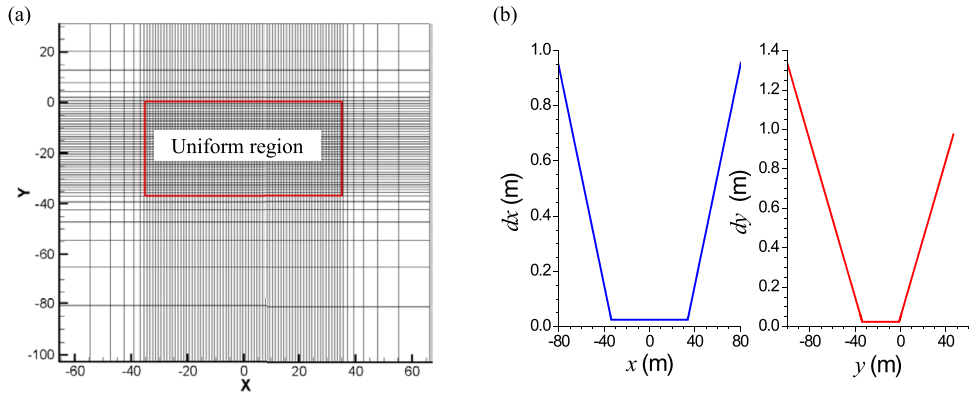

FIG. 9. Mesh strategy of the fluid domain; every one in 20 of the lines is plotted in the left figure (a) and grid length distribution of two normal directions is plotted in the right figure (b).

III. NUMERICAL RESULTS

A. Cavitation induced by small-charge explosions at shallow water depths in the 2D plane model

In this section, we first consider two charges placed horizontally in underwater explosions near free surfaces, as shown in Fig. 1. Here, the distance (H_0) between the charge center and water surface is 1.0 m, and the initial radius (R_0) of the charge is set to 0.04 m, which is similar to the cross section of 0.5 kg spherical 2,4,6-trinitrotoluene [C7H5(NO2)3] (TNT) charge in the 2D computational domain. The mesh strategy has been shown in Fig. 2, where non-uniform grids are used in both x and y directions. The four cases with different

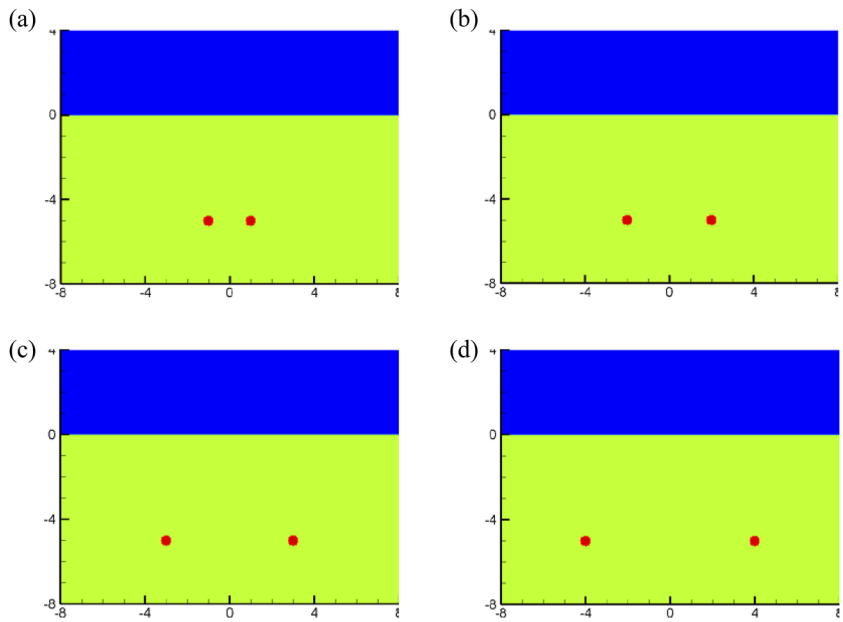

FIG. 10. Schematic of the two-charge underwater explosion at 1 m detonation depth with different distances: (a) L_0 = 2 m; (b) L_0 = 4 m; (c) L_0 = 6 m; (d) L_0 = 8 m.

distances of L_0 = 0.5, 1.0, 1.5, and 2.0 m are simulated in this section, as shown in Fig. 3. Meanwhile, another case of single charge placed on the y axis with R_0 = 0.04 m and H_0 = 1.0 m is also simulated as the basic comparison.

Figure 4 displays the numerical results of density contour plots at six different times t = 1.55, 3.22, 7.29, 8.90, 16.2, and 24.3 ms (from left to right)—different underwater conditions. It is found that the maximum volume of each explosion bubble in two-charge cases is smaller than that of the single charge case at the same time. This is mainly due to the fact that the two explosion bubbles would inhibit each other in the two-charge cases, which hinders the normal expansion velocity of the bubbles. The rarefaction wave is reflected near the free surface under the condition of single charge exploded near the free surface. Therefore, the cavitation mainly occurs in a narrow area near the free surface under water, as shown in the single case in Fig. 4. It is found that there is a narrow area with low density under the free surface, which is closely related to the occurrence of cavitation. In order to further investigate these areas of abnormal density, the numerical results of the vapor volume fraction contour plots are shown in Fig. 5. It is found that in the interaction between the shock wave and free surface, not only the rarefaction wave reflected from the free surface will produce a vapor zone in water but also the water will be evaporated from the free surface and spread into the air when the compression wave is transmitted to the air domain. The vapor volume fraction diffused into the air is generally greater than 0.8. In addition, for the vapor volume fraction in water, the area where the vapor volume fraction is greater than 0.0005 in the numerical results is close to the cavitation domain observed in the experiment (Yu *et al.*, 2022). Therefore, Fig. 6 shows the numerical results of the cavitation domain contour plots under different conditions. The red zones represent the cavitation area, and the green, blue, and light blue color zones are air, water and the explosion bubble, respectively. It is found that there are obvious differences between the single charge and two charges with different distances. With the increase in the number of charges, the area of the cavitation domain did not increase accordingly but decreases significantly. This is because when the cavitation domain produced by one of the charges begins to increase, the shock wave generated by the other charge may have just arrived. Therefore, the shock wave produced by the two charges has an important

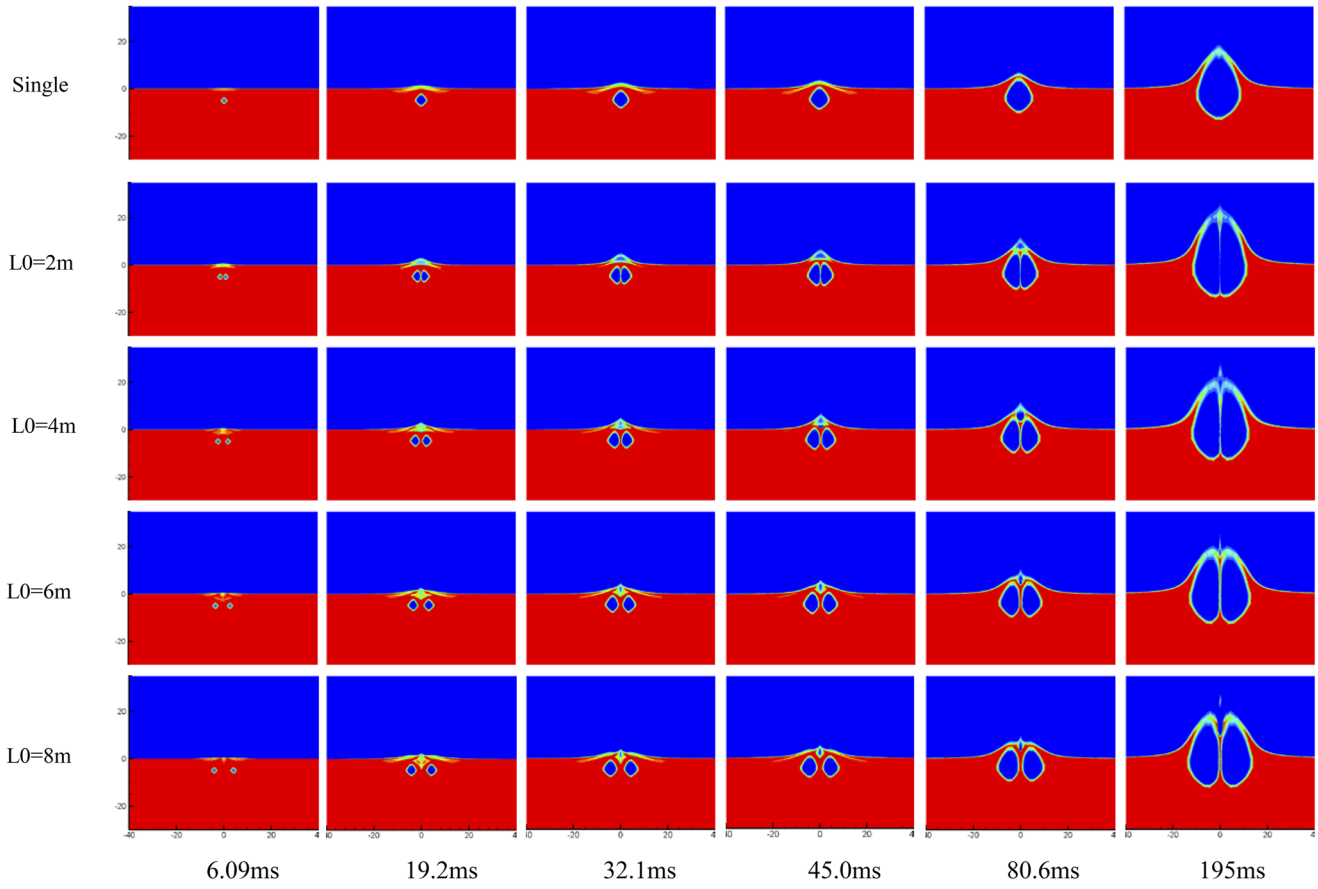

FIG. 11. Numerical results of the density contour plot at times of t = 6.09, 19.2, 32.1, 45.0, 80.6, and 195 ms (from left to right) at R_0 = 0.25 m and H_0 = 5 m in the cases of single charge and two charges with different detonation distances L_0 (from up to down).

inhibitory effect on each other's cavitation domain, which affects the normal evolution process of the cavitation domain produced by each other.

Figure 7 shows the time-history of the cavitation domain area in different cases. It is found that the cavitation area induced by two charges is generally smaller than that induced by a single charge. The evolution of cavitation produced by two charges is much earlier than that by a single charge, including the moment of the maximum cavitation occurrence and cavitation collapse. Figure 8 shows the pressure time history curve for the location of (0, −0.2) m at the shock wave stage and cavitation stage. It can be observed that the peak pressure increases from 87.3 MPa of the single charge case to 198.8 MPa of the two-charge case. The peak pressure of the shock wave under two charges is 2.28 times that of the single charge case, which shows that there is no linear superposition effect of shock wave pressure in underwater explosions. It is found that there are many high frequency components in the pressure curve at the cavitation stage, which can be attributed to the strong nonlinear interactions between the cavitation flow and surrounding water.

B. Cavitation induced by the big-charge exploded at deeper water in the 2D plane model

In order to investigate the effect of charge quality and detonation depth on the cavitation evolution of two charges in underwater explosions, the underwater explosion induced by the big charge exploded at deep water depth is simulated by the two-dimensional (2D) plane model, as shown in Fig. 1. The distance (H_0) between the charge center and water surface is 5.0 m, and the initial radius (R_0) of the charge is set to 0.25 m, which is similar to the cross section of 100 kg spherical TNT charge in the 2D computational domain. Here, the mesh strategy has been shown in Fig. 9, where non-uniform grids are used in both x and y directions. The four cases with different distances of L_0 = 2, 4, 6, and 8 m are simulated in this section, as shown in Fig. 10. Meanwhile, another case of a single charge placed on the y axis with R_0 = 0.25 m and H_0 = 5 m is also simulated as the basic comparison.

Figure 11 depicts the numerical results of the density contour plot at six different times t = 6.09, 19.2, 32.1, 45.0, 80.6, and 195 ms (from left to right)—different underwater conditions. It is also found

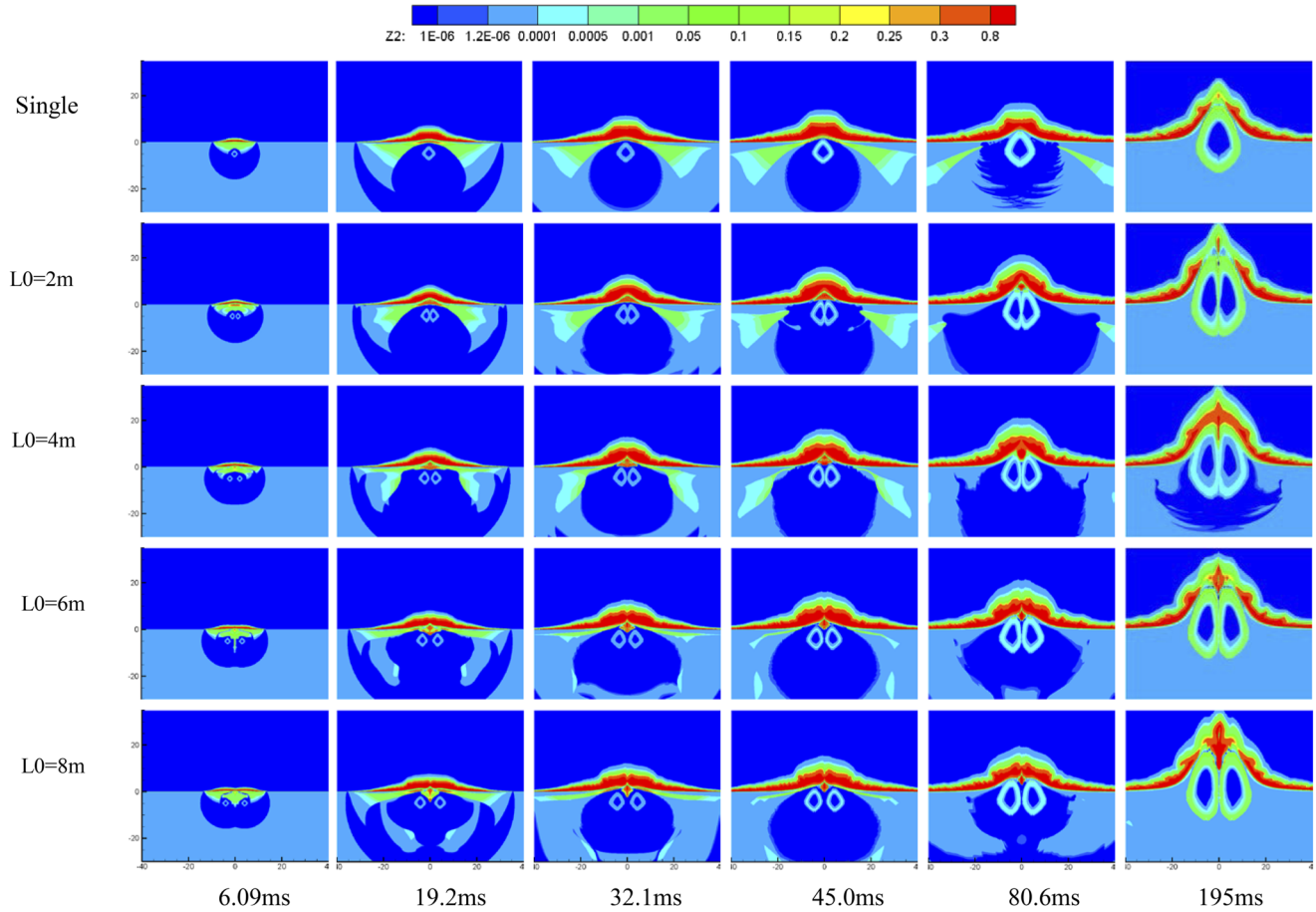

FIG. 12. Numerical results of the vapor volume fraction contour plot at times of t = 6.09, 19.2, 32.1, 45.0, 80.6, and 195 ms (from left to right) at R_0 = 0.25 m and H_0 = 5 m in the cases of single charge and two charges with different detonation distances L_0 (from up to down).

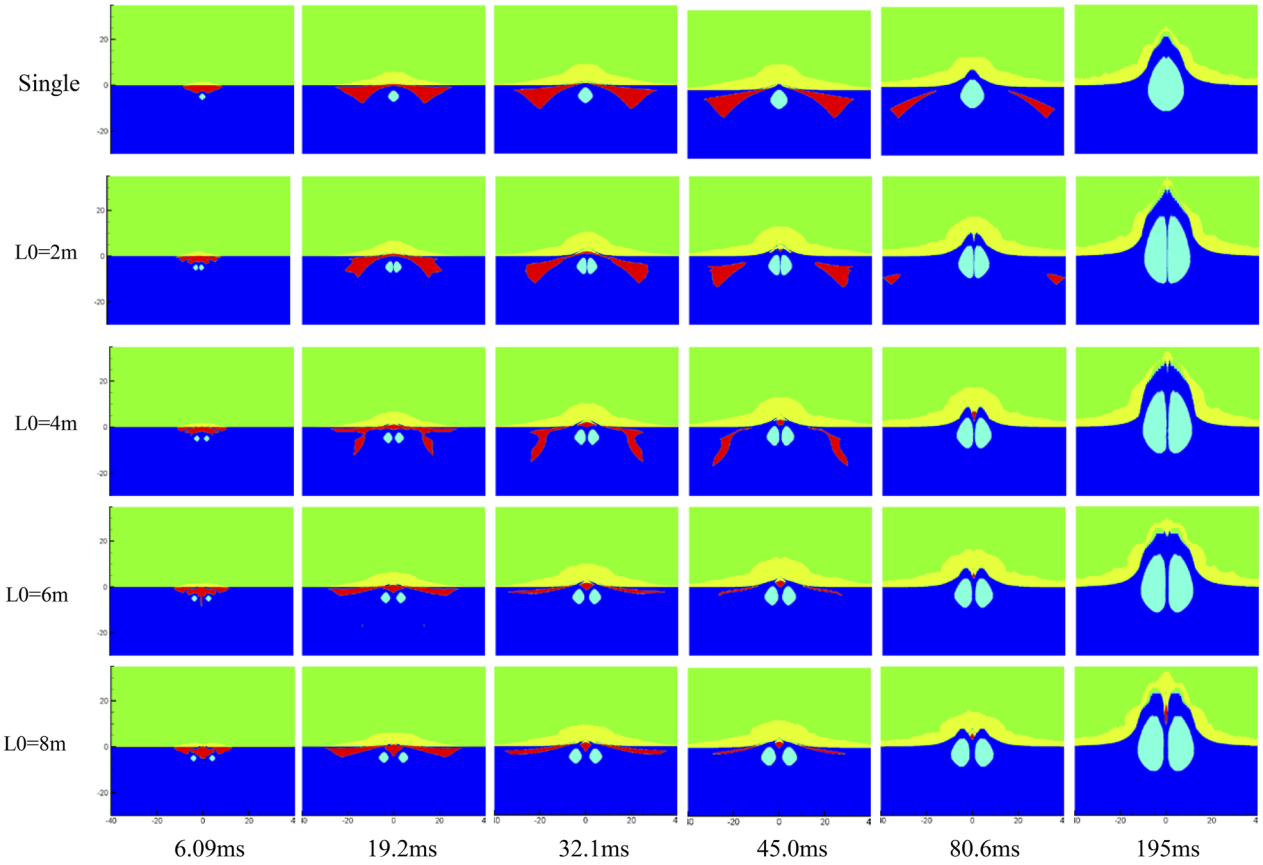

FIG. 13. Numerical results of the cavitation domain contour plot at times of t = 6.09, 19.2, 32.1, 45.0, 80.6, and 195 ms (from left to right) at R_0 = 0.25 m and H_0 = 5 m in the cases of single charge and two charges with different detonation distances L_0 (from up to down).

that the maximum volume of each explosion bubble in two charges cases is smaller than that in the single charge case at the same time. Figures 12 and 13 show the numerical results of the vapor volume fraction and cavitation domain contour plots in the same cases. With the increase in the charge weight and detonation depth, the evolution of the cavitation domain becomes more complex than that shown in Fig. 6. It is found from the cases of L_0 = 2 m and L_0 = 4 m in Fig. 13 that the cavitation domain has expanded to the area much deeper than the explosion bubble location rather than just staying near the free surface. This phenomenon must be paid enough attention because it will have an important influence on the input load of underwater structures. The cavitation evolution of the case of "single" and "L_0 = 2 m" cases is similar in terms of the overall trend. In the process of expansion and subsequent evolution of the cavitation domain, the cavitation in the region near the y-axis first collapses, and then the cavitation domain is gradually flattened and diffused to both sides. For the other three cases with different distances between the two charges, the shock wave will also produce a rarefaction wave as it reaches the interface of the explosion bubble. Therefore, it can be observed that there is some cavitation in the middle of the two explosion bubbles at the initial stage. In addition, the cavitation does not collapse from the middle region at first, but the whole cavitation domain gradually shrinks. Under the condition of big charge underwater explosions at deeper water, the occurrence area of cavitation is very large, and its harm to the surrounding structures is much more serious.

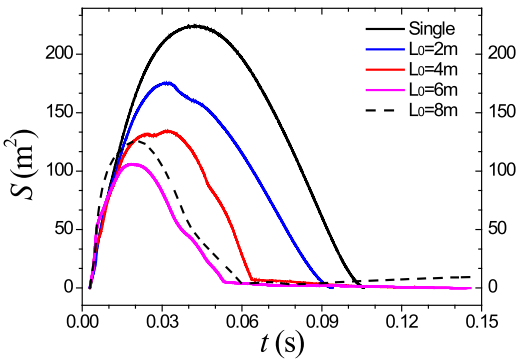

FIG. 14. Time-history curve of cavitation domain volume evolvement at R_0 = 0.25 m and H_0 = 5 m in the cases of single charge and two charges with different detonation distances L_0.

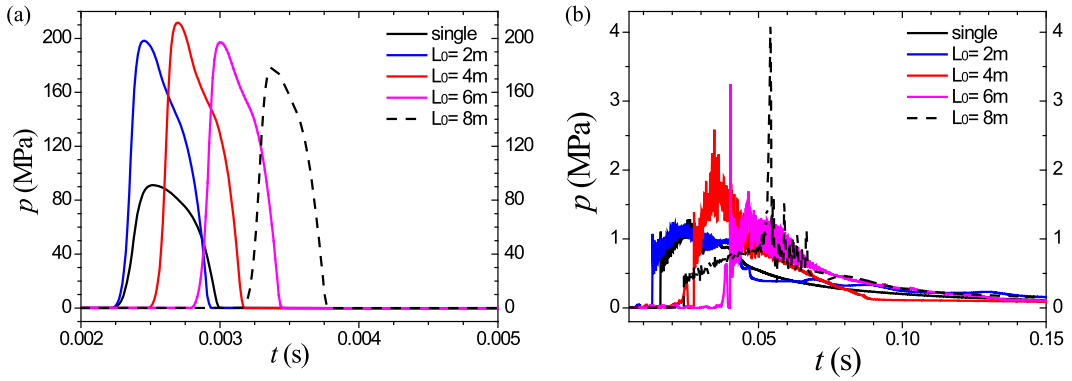

FIG. 15. Pressure time-history curves for the location of (0, −0.5) m at R_0 = 0.25 m and H_0 = 5 m in the cases of single charge and two charges with different detonation distances L_0. (a) The pressure at the shock wave stage. (b) The pressure at cavitation pressure curve.

Figure 14 shows the time-history of the cavitation domain area for different cases. It is also found that the cavitation area induced by two charges is generally smaller than that induced by the single charge. The evolution of cavitation produced by two charges is much earlier than that by the single charge, including the moment of the maximum cavitation occurrence and cavitation collapse. Figure 8 shows the pressure time history curve for the location of (0, −0.5) m at the shock wave stage and cavitation stage. It can be observed that the peak pressure increases from 91.1 MPa of the single charge case to 211.4 MPa of the two-charge case. The peak pressure of the shock wave under two charges is 2.32 times that under the single charge case, which also shows that there is no linear superposition effect of shock wave pressure in underwater explosions. For the pressure in the cavitation stage shown in Fig. 15(b), the peak pressure after excluding the high frequency component is within 1–2 MPa range. Although the pressure amplitude is low, the effective action time is basically longer than 10 ms, while it is only about 1 ms in the shock wave stage shown in Fig. 15(a).

C. Cavitation induced by the big-charge exploded at deep water depth in the 2D axisymmetric model

In this section, the cavitation effect induced by two big charges placed vertically is studied quantitatively by the two-dimensional (2D) axisymmetric model in underwater explosions at deep water depth, as shown in Fig. 16. The initial radius (R_0) of the charge is set to 0.25 m, which corresponds to the 100 kg spherical TNT explosive. The distances H_1 and H_2 are set to 5 m. Here, the mesh strategy has been shown in Fig. 17, where non-uniform grids are used in both x and y directions.

Figure 18 reveals the numerical results of the density, pressure, vapor volume fraction, and cavitation domain contour plot (from up to down) at times of t = 13.1, 34.9, 60.8, and 73.8 ms (from left to right). It is found from the density plots that the two explosion bubbles begin to merge as the single bubble expands. The volume of the cavitation domain reaches its maximum, and a high-pressure zone appears around the explosion bubble at 34.9 ms. With the continuous advancement of the high-pressure zone to the cavitation domain, the cavitation volume is squeezed and gradually decreases at 60.8 and 73.8 ms. Figure 19 shows the numerical results at times of t = 104, 135, 165, and 200 ms, which corresponds to the stage of the explosion bubble motion. With the continuous expansion of the bubbles, the interface between the two gradually disappears and finally completely merges into a complete bubble.

Figure 20 shows the time-history of the cavitation domain. The evolution of the cavitation domain shows the detailed expansion stage and contraction stage, and the duration of these two stages is basically the same, which seems to be very similar to the pulsating process of explosion bubbles under water. Figure 21 shows the pressure time history curve at the four locations closer to the free surface in the horizontal direction. The peak pressure decreases

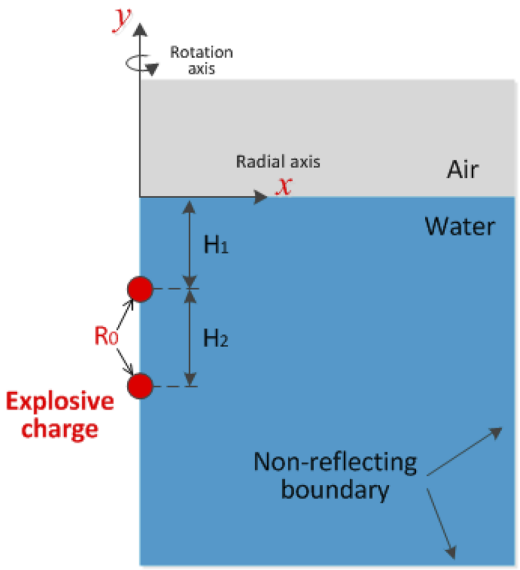

FIG. 16. Schematic diagram of two charges placed vertically in underwater explosions.

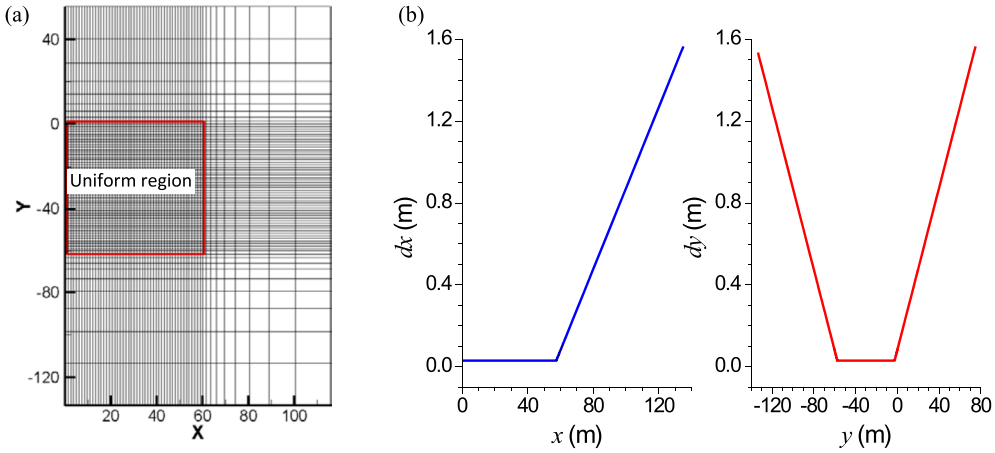

FIG. 17. Mesh strategy of the fluid domain; every one in 20 of the lines is plotted in the left figure (a) and grid length distribution of two normal directions is plotted in the right figure (b).

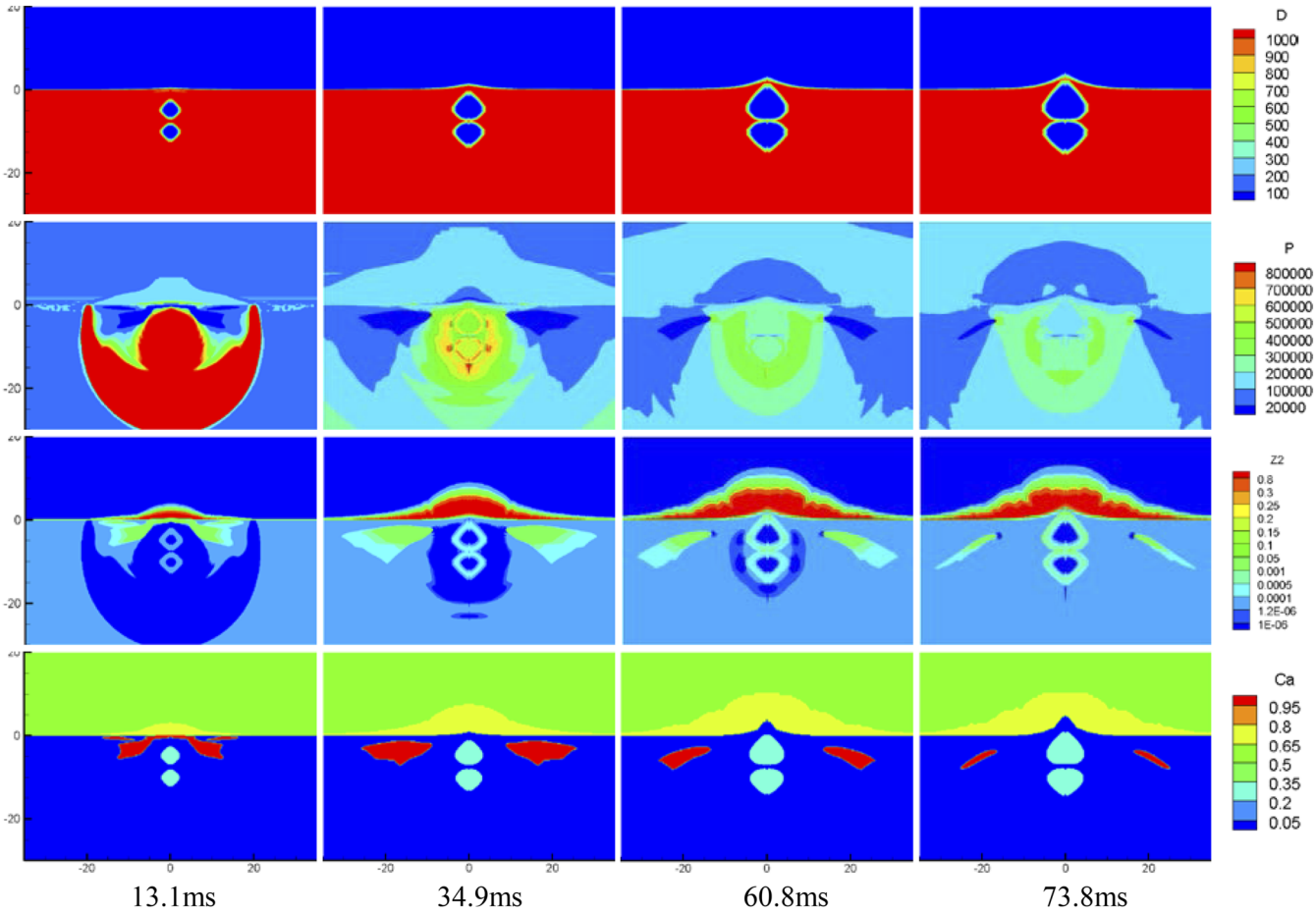

FIG. 18. Numerical results of the density, pressure, vapor volume fraction, and cavitation domain contour plot (from up to down) at times of t = 13.1, 34.9, 60.8, and 73.8 ms (from left to right) at R_0 = 0.25 m, H_1 = 5 m, and H_2 = 5 m.

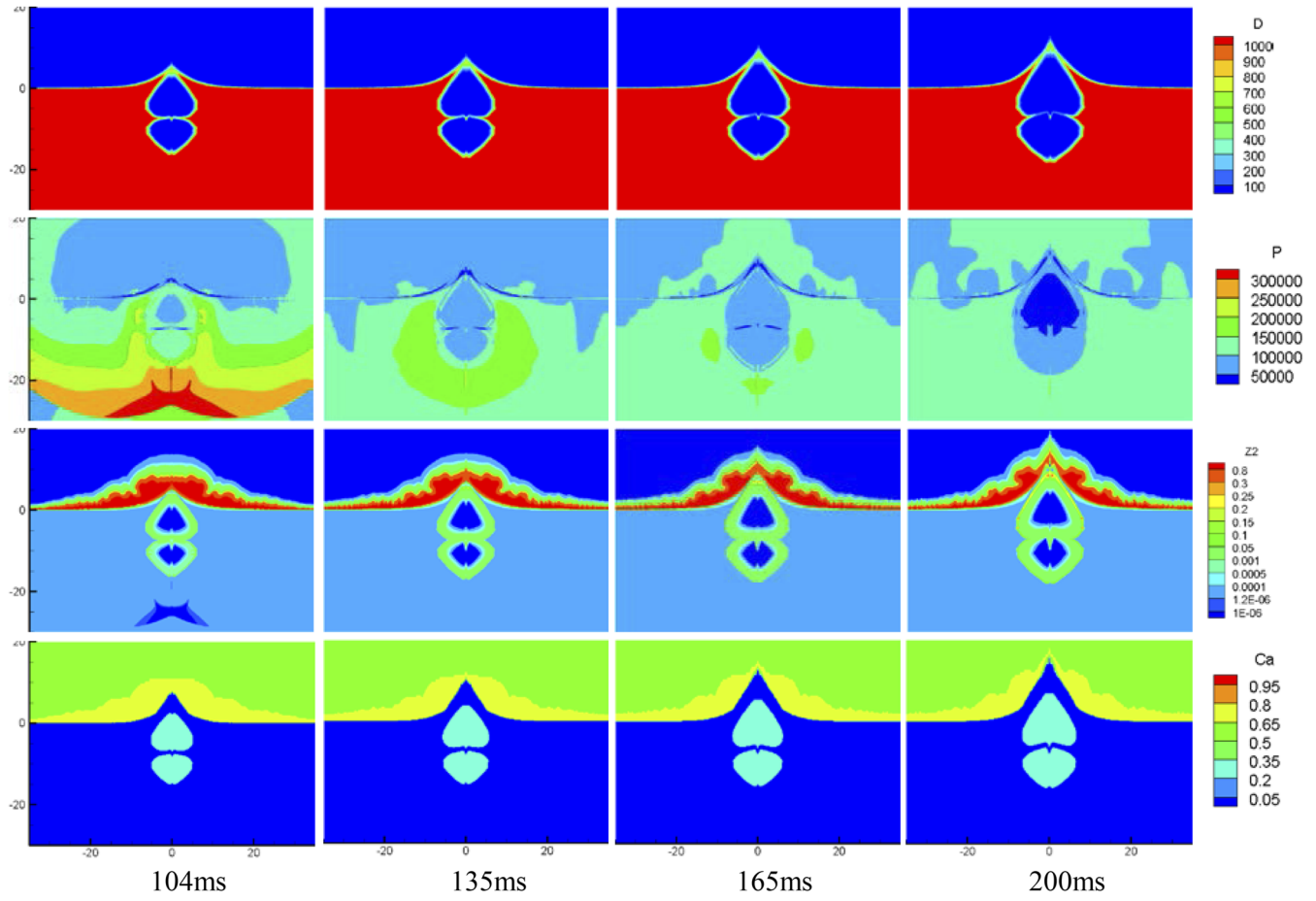

FIG. 19. Numerical results of the density, pressure, vapor volume fraction, and cavitation domain contour plot (from up to down) at times of t = 104, 135, 165, and 200 ms (from left to right) at R_0 = 0.25 m, H_1 = 5 m, and H_2 = 5 m.

gradually with the increase in the distance between the measuring point and the charges in the shock wave stage shown in Fig. 21(a). However, this algorithm does not apply to the pressure characteristics in the cavitation stage. It is found that the maximum pressure occurs at the location of (4, −0.5) m and the peak pressure value is 7.26 MPa. Meanwhile, the cavitation pressure characteristic of this point is quite different from others. The peak pressure at this point is large, but the effective time is short, while the peak pressure at other points is small, but the effective time is long. In order to investigate the mechanics of this phenomenon, the numerical results of pressure and cavitation domain contour plots are shown in Fig. 22. It is found that the cavitation located on the y-axis begins to collapse and the cavitation domain moves to both sides at 17.4 ms. However, high pressure zones appear on both sides and spread to the outside at 19.6 ms, which corresponds to the measuring point (4, −0.5) m in Fig. 21.

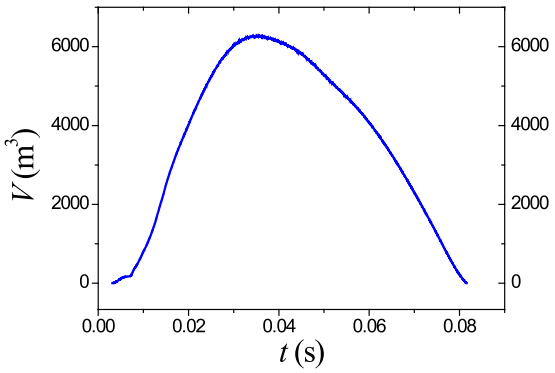

FIG. 20. Time-history curve of cavitation domain volume evolvement at R_0 = 0.25 m, H_1 = 5 m, and H_2 = 5 m.

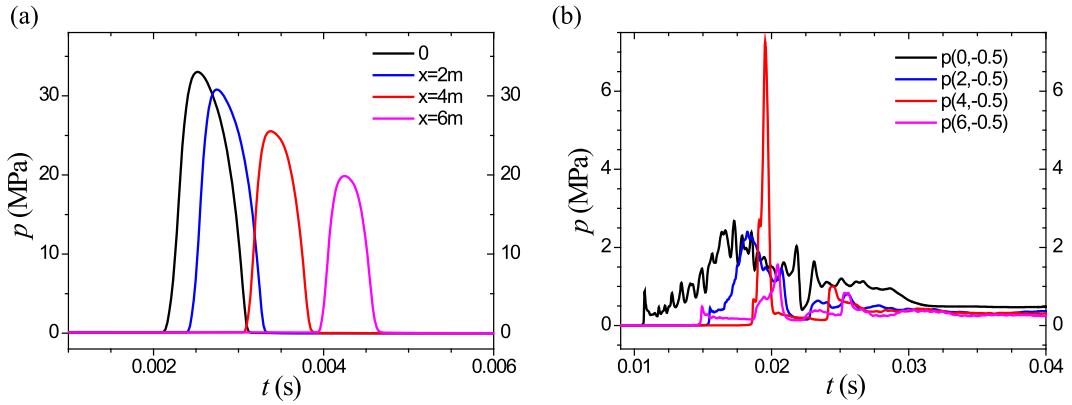

FIG. 21. Pressure time-history curves of four locations at R_0 = 0.25 m and H_0 = 5 m. (a) The pressure at the shock wave stage. (b) The pressure at cavitation stage.

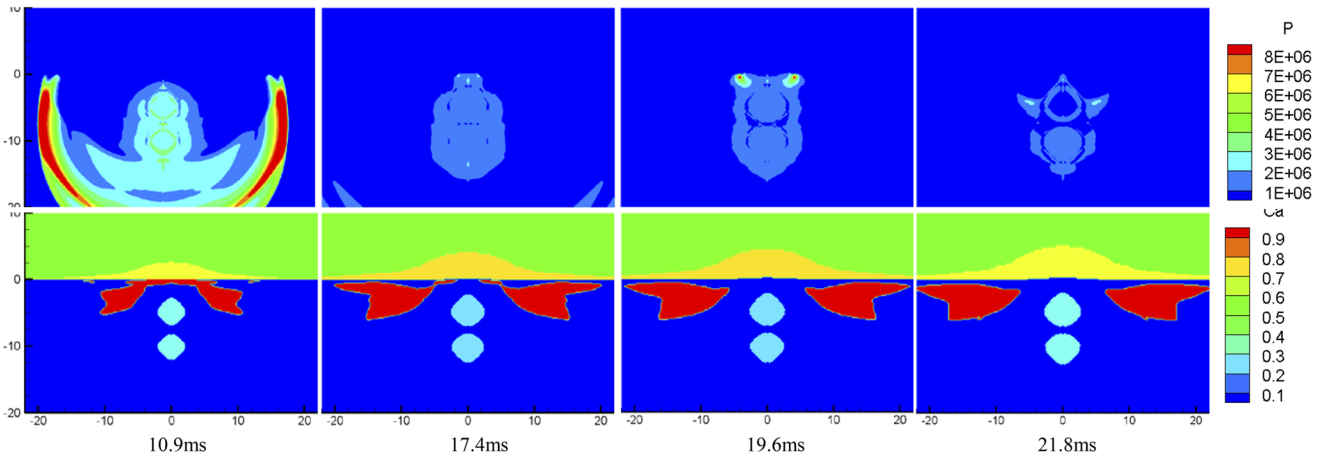

FIG. 22. Numerical results of the pressure and cavitation domain contour plot (from up to down) at times of t = 10.9, 17.4, 19.6, and 21.8 ms (from left to right).

IV. CONCLUSIONS

In this paper, the strong nonlinear interaction between the two charges and cavitation is numerically researched by a four-equation system with a phase transition model to understand the cavitation effect in underwater explosions near free surfaces. A two-dimensional plane model is used to qualitatively study the two charges placed horizontally with different charge radii R_0 and detonation depths H_0. Numerical results show that not only the rarefaction wave reflected from the free surface will produce a vapor zone in water but also the water will be evaporated from the free surface and spread into the air when the compression wave is transmitted to the air domain. The vapor volume fraction diffused into the air is generally greater than 0.8. This is because when the cavitation domain produced by one of the charges begins to increase, the shock wave generated by the other charge may have just arrived. Therefore, the shock wave produced by two charges has an important inhibitory effect on each other's cavitation domain, which affects the normal evolution process of the cavitation domain produced by each other. Meanwhile, a two-dimensional axisymmetric model is adopted to quantitatively investigate the two charges placed vertically. It is found from the numerical results that the peak value of the cavitation pressure can reach 7.26 MPa and that the algorithm of pressure distribution in the shock wave stage is quite different from that in the cavitation stage. The occurrence of the generation, development, and collapse of cavitation can be captured directly in all the numerical cases.

This study investigates the cavitation effect induced by two charges in underwater explosions near free surfaces. The complex interaction between these multiphase fluids with the surrounding structures is an interesting topic for future studies.

AUTHOR DECLARATIONS

Conflict of Interest

The authors have no conflicts to disclose.

Author Contributions

Jun Yu: Conceptualization (equal); Methodology (equal); Software (equal); Writing – original draft (equal). **Hai-tao Li**: Data curation (equal); Methodology (equal); Writing – review & editing (equal). **Zhen-xin Sheng**: Project administration (equal); Visualization (equal); Writing – review & editing (equal). **Yi Hao**: Formal analysis (equal); Methodology (equal); Visualization (equal). **Jian-hu Liu**: Conceptualization (equal); Methodology (equal); Project administration (equal).

DATA AVAILABILITY

The data that support the finding of this study are available from the corresponding author upon reasonable request.

REFERENCES

[1] R. H. Cole, *Underwater Explosion* (Princeton University Press, NJ, 1948), pp. 3–8.
[2] J. J. Esplin, "Bulk cavitation extent modeling: An energy-based approach," Doctor's Thesis, 2016, pp. 1–8.
[3] J. H. Liu, "Theory and its applications of ship dynamic responses to non-contact underwater explosions," Doctor's Thesis, wuxi CSSRC, China, 2002 5–8.
[4] J. Yu, G.-z. Liu, J. Wang, and H.-k. Wang, "An effective method for modeling the load of bubble jet in underwater explosion near the wall," Ocean Eng. **220**, 108408 (2021).
[5] W. B. Gu, B. L. Sun, T. H. Yang *et al.*, "Numerical simulation of explosive shock wave interaction in shallow-layer water," J. PLA Univ. Sci. Technol. **4**(6), 64–68 (2003).
[6] S. Rungsiyaphornrat, E. Klaseboer, B. C. Khoo, and K. S. Yeo, "The merging of two gaseous bubbles with an application to underwater explosions," Comput. Fluid **32**, 1049–1074 (2003).
[7] S. Li, A.-M. Zhang, R. Han, and P. Cui, "Experimental and numerical study of two underwater explosion bubbles: Coalescence, fragmentation and shock wave emission," Ocean Eng. **190**, 106414 (2019).
[8] H. W. Hu, P. Song, S. F. Guo, H. Y. Feng, and D. K. Li, "Shock wave and bubble characteristics of underwater array explosion of charges," Defence Technol. **18**(8), 1445–1453 (2021).
[9] Z.-w. Hou, N. Li, X.-l. Huang *et al.*, "Three-dimensional numerical simulation on near-field pressure evolution of dual-tube underwater detonation," Phys. Fluids **34**, 033304 (2022).
[10] T.-H. Phan, V.-T. Nguyen, and W.-G. Park, "Numerical study on strong nonlinear interactions between spark- generated underwater explosion bubbles and a free surface," Int. J. Heat Mass Transfer **163**, 120506 (2020).
[11] Y. Chen and S. D. Heister, "A numerical treatment for attached cavitation," J. Fluid Eng. **116**, 613–618 (1994).
[12] D. P. Schmidt, C. J. Rutland, and M. L. Corradini, "A fully compressible, two-dimensional model of small, high speed, cavitating nozzles," Atomization Sprays **9**, 255–276 (1999).
[13] T. G. Liu, B. C. Khoo, and W. F. Xie, "Isentropic one-fluid modelling of unsteady cavitating flow," J. Comput. Phys. **201**, 80–108 (2004).
[14] W. F. Xie, T. G. Liu, and B. C. Khoo, "Application of a one-fluid model for large scale homogeneous unsteady cavitation: The modified Schmidt model," Comput. Fluids **35**, 1177–1192 (2006).
[15] A. Daramizadeh and M. R. Ansari, "Numerical simulation of underwater explosion near air-water free surface using a five-equation reduced model," Ocean Eng. **110**, 25–35 (2015).
[16] M. Pelanti and K.-M. Shyue, "A mixture-energy-consistent six-equation two-phase numerical model for fluid with interfaces, cavitation and evaporation waves," J. Comput. Phys. **259**, 331–357 (2014).
[17] M. Pelanti and K.-M. Shyue, "A numerical model for multiphase liquid-vapor-gas flows with interfaces and cavitation," Int. J. Multiphase Flow **113**, 208–230 (2019).
[18] A. Chiapolino, P. Boivin, and R. Saurel, "A simple phase transition relaxation solver for liquid–vapor flows," Int. J. Numer. Methods Fluids **83**(7), 583–605 (2016).
[19] A. Chiapolino, P. Boivin, and R. Saurel, "A simple and fast phase transition relaxation solver for compressible multicomponent two-phase flows," Comput. Fluids **150**, 31–45 (2017).
[20] J. Yu, J.-h Liu, B. He, H.-t Li, T. Xie, and D. Pei, "Numerical research of water jet characteristics in underwater explosion based on compressible multicomponent flows," Ocean Eng. **242**, 110135 (2021).
[21] J. Yu, J.-h. Liu, H.-k. Wang, J. Wang, L.-p. Zhang, and G.-z. Liu, "Numerical simulation of underwater explosion cavitation characteristics based on phase transition model in compressible multicomponent fluids," Ocean Eng. **240**, 109934 (2021).
[22] J. Yu, J.-h. Liu, H.-k. Wang, J. Wang, Z.-t. Zhou, and H.-b. Mao, "Application of two-phase transition model in underwater explosion cavitation based on compressible multiphase flows," AIP Adv. **12**, 025209 (2022).
[23] J. Yu, W.-W. Wu, B. Yan, J.-T. Dong, X.-P. Zhang, and H. B. Mao, "Study on the mechanism and load characteristics of secondary cavitation near free surface in underwater explosion," AIP Adv. **12**, 105222 (2022).
[24] J. Zhang, "A simple and effective five-equation two-phase numerical model for liquid-vapor phase transition in cavitating flows," Int. J. Multiphase Flow **132**, 103417 (2021).
[25] O. Le Métayer and R. Saurel, "The Noble-Abel stiffened-gas equation of state," Phys. Fluids **28** (4), 046102 (2016).